

---

Journal of the  
STRUCTURAL DIVISION  
Proceedings of the American Society of Civil Engineers

---

SEISMIC RESISTANCE OF REINFORCED CONCRETE  
BEAM-COLUMN JOINTS

By Norman W. Hanson,<sup>1</sup> and Harold W. Connor,<sup>2</sup>

---

INTRODUCTION

The ability of multistory reinforced concrete frames to resist violent earthquakes has been demonstrated in Chile (1960), Yugoslavia (1963), and Alaska (1964). Comprehensive reports<sup>3,4,5</sup> of structural performance during these shocks have verified recommendations for earthquake design and reinforcement details. Primary structural members such as beams, columns and slabs developed adequate resistance to seismic forces. Where unsatisfactory performance was observed, it could usually be attributed to quality of materials or construction, or to poor reinforcement details in the structural joints.

A book by J. A. Blume *et al.*,<sup>6</sup> hereafter referred to as the Earthquake Manual, contains recommendations for design of reinforced concrete structures that provide ductility and strength to resist major earthquakes. Crucial recommendations for earthquake resistant design are the following:

Note.—Discussion open until March 1, 1968. To extend the closing date one month, a written request must be filed with the Executive Secretary, ASCE. This paper is part of the copyrighted Journal of the Structural Division, Proceedings of the American Society of Civil Engineers, Vol. 93, No. ST5, October, 1967. Manuscript was submitted for review for possible publication on September 14, 1966.

<sup>1</sup>Sr. Development Engr., Structural Development Sect., Research and Development Div., Portland Cement Assoc., Skokie, Ill.

<sup>2</sup>Development Engr., Structural Development Sect., Research and Development Div., Portland Cement Assoc., Skokie, Ill.

<sup>3</sup>"The Behavior of Reinforced Concrete Buildings Subjected to the Chilean Earthquakes of May 1960," Advanced Engineering Bulletin No. 6, Portland Cement Association, Skokie, Ill.

<sup>4</sup>Kunze, W. E., Fintel, M., and Amrhein, J. E., "Skopje Earthquake Damage," Civil Engineering, Dec., 1963.

<sup>5</sup>Kunze, W. E., Sbarounis, J. A., and Amrhein, J. E., "The March 27 Alaskan Earthquake—Effects on Structures in Anchorage," Journal of the American Concrete Institute, Detroit, Mich., June, 1965, pp. 635-649.

<sup>6</sup>Blume, J. A., Newmark, N. M., and Corning, L. H., Design of Multi-Story Reinforced Concrete Buildings for Earthquake Motions, Portland Cement Association, Skokie, Ill., 1961, pp. 318.

1. Sufficient transverse or shear reinforcement to provide a shear strength greater than the flexural strength.

2. Limitations on the amount of tensile reinforcement, or required use of compression reinforcement, to ensure ductility and energy-absorbing capacity.

3. Confinement of the concrete by hoops or spirals at critical sections, such as beam-column connections, to increase the ductility of columns under combined axial load and bending.



FIG. 1.—SPECIMEN READY FOR TEST

4. Special attention to details, such as splices in reinforcement and exclusion of planes of weakness that would result from bending or terminating all bars at the same section.

*Purpose and Scope.*—To verify the above recommendations, the Structural Engineers Association of California (SEAO) Seismology Committee suggested that tests be conducted on a series of full-size specimens. The purpose of this investigation was to determine joint reinforcement required to ensure maintaining ultimate capacity for cast-in-place beams and columns

subjected to multiple reversals of loading of major earthquake magnitude.

The principal variables of this study were column-size, column load, and degree of confinement of concrete in the joint. An exterior column and beam joint was selected for study. This is the most critically loaded joint in a multistory building. A series of six specimens of the type shown in Fig. 1 were tested. Two column sizes and two amounts of hoop reinforcement in the joint were included. Identically designed specimens were tested under two levels of column load. A seventh specimen with short spandrel beam stubs was also tested. This represented a less critical joint, since the connection was confined on two sides by surrounding concrete members.

## EARTHQUAKE DESIGN CONCEPTS

In the Earthquake Manual,<sup>6</sup> it is stated that a building frame should be proportioned so that a structure will resist a moderate earthquake without damage, and will survive the most severe earthquake reasonably predictable during the life of the building, without major structural damage. Furthermore, the structure should not collapse even when subjected to the motions of an earthquake of abnormal intensity. It is assumed, or course, that no structure would be located directly over an active known fault.

The usual procedures of earthquake-resistant design<sup>7</sup> are based on the premise that strong ground motion may cause local overstressing, but that ductility is sufficient to dissipate the energy of the vibrations without danger of collapse. Earthquake design recommendations recognize that absorption of seismic energy is best satisfied by flexural yielding. Therefore, provisions are made to restrict compression or shear weaknesses, stress concentrations, and joint brittleness.

### Definitions.

**Rotational Ductility**—the ability of a flexural member to continue sustaining plastic rotations without rupture. The ductility factor,  $\mu$ , is the ratio of the rotation at ultimate load to the rotation at yield load.

**Plastic Hinge**—a zone of yielding due to flexure in a structural member. Although a hinge has a finite length that depends on both geometry and loading, it is assumed in most analytical work that all plastic rotation occurs at a single plane section. For this study, the length of the hinging zone was assumed to be equal to one-half the beam depth. In structures where plastic hinges occur, the member continues to rotate about the hinged section at a nearly constant restraining moment.

**Moment-Rotation Curve**—for a reinforced concrete flexural member can be compared to the stress-strain curve for a steel with a definite yield. The member behaves elastically up to the yield point which for underreinforced members corresponds to computed yield in the tensile steel reinforcement. Subsequent deformation at the plastic hinge permits an increase in rotation with little increase in applied moment.

**Earthquake Representation.**—Although the response of a multistory building to dynamic deformations caused by an earthquake is a complex phenomenon,

<sup>7</sup>Housner, G. W., "The Plastic Failure of Frames During Earthquakes," *Proceedings, Second World Conference on Earthquake Engineering*, Vol. 11, 1960, Tokyo, Japan, pp. 997-1012.

reinforcing steel yield stress), and  $k_1 = 0.85$  (a factor depending on  $f'_c$ ). For ductility as an earthquake resistant structure, maximum reinforcement ratio of 0.025 is suggested in the Earthquake Manual. This reinforcement ratio has been shown<sup>13</sup> to provide considerable ductility. Therefore, 4 No. 9 bars at effective depth,  $d$ , of 17.56 in. were selected as the top reinforcement to resist the negative moment. This provided a reinforcement ratio  $\rho = 0.019$ . Two No.

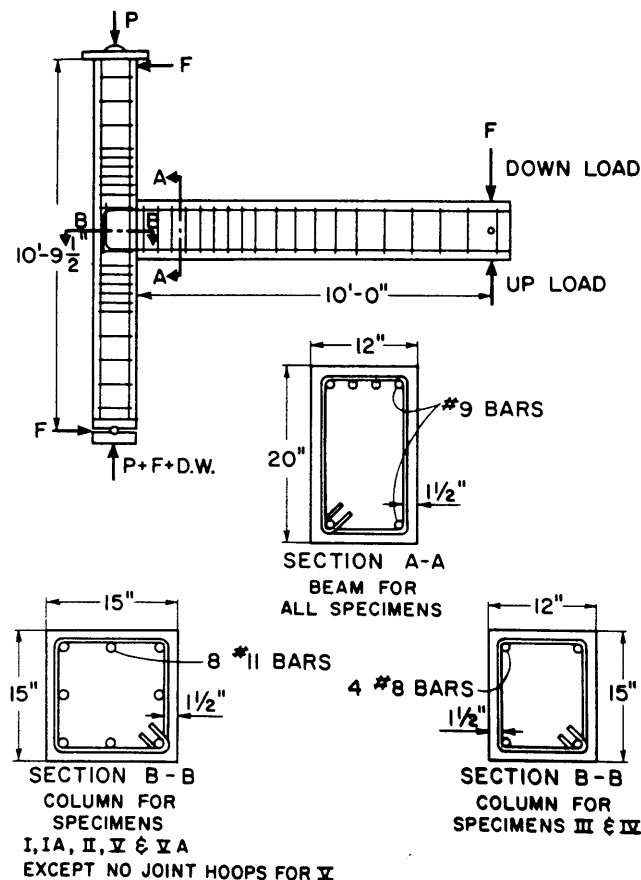


FIG. 4.—BEAM-COLUMN DETAILS

9 bars were selected as bottom reinforcement to resist the positive moment, so that  $\rho' = 0.0095$ .

Since the beam compression reinforcement does not yield as shown by ACI 318-63 Eq. (16-4), ultimate design resisting moments,  $M_u$ , were computed by Eq. (16-1) with the capacity reduction factor,  $\phi$ , equal 1.0, since material properties and loading are known so that

<sup>13</sup>Ernst, G. C., "Plastic Hinging at the Intersection of Beams and Columns" *Journal of the American Concrete Institute*, Detroit, Mich., Vol. 53, June, 1957, pp. 1119-1144.

$$M_u = b d^2 f'_c q (1 - 0.59 q) \quad (2a)$$

$$\text{in which } q = A_s f_y / b d f'_c = 0.253 \quad (2b)$$

for negative moment and 0.127 for positive moment. These ultimate moments were 199 ft-kips and 109 ft-kips for negative and positive moment, respectively.

In the 120-in. shear region between beam load and column face, total ultimate shear was 19.9 kips. Web reinforcement was not required by ACI 318-63 for this shear. For seismic loadings, however, the Earthquake Manual

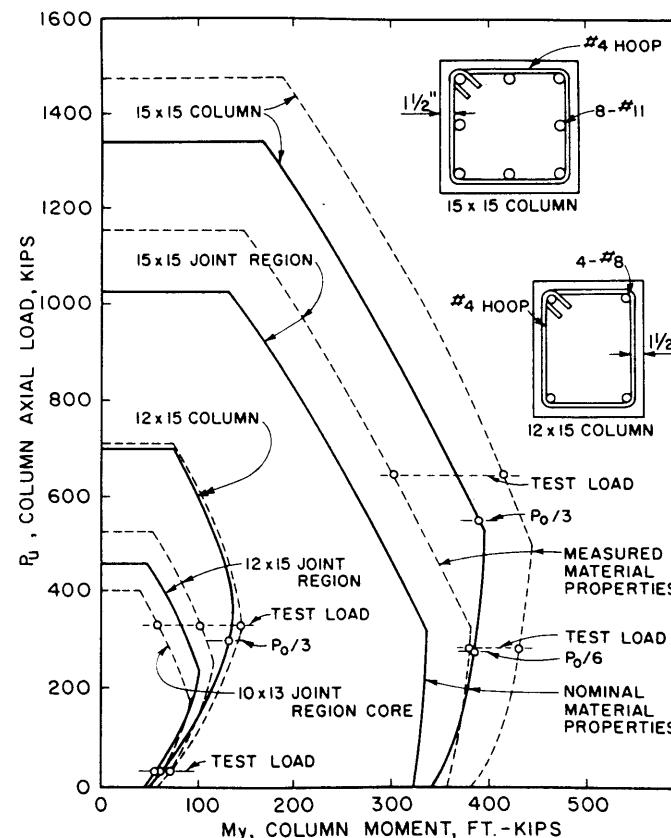


FIG. 5.—COLUMN LOAD—MOMENT INTERACTION CURVES

recommends closed stirrups (stirrup-ties) within a distance equal to four times the effective beam depth from the column face, not less than

$$A_v = 0.15 A_s s / d \quad (3)$$

in which  $A_v$  = total area of web reinforcement within a distance  $s$ , crossing a plane parallel to the longitudinal reinforcement, and  $A_s$  = area of tension reinforcement. No. 3 stirrup-ties were provided at 4.5-in. spacing ( $d/4$ ) over

rams were assembled in three parallel sets and the upload rams in two parallel sets.

Prior to application of load to the beam, axial thrust was applied to the column by the testing machine. The down-load portion of a beam loading cycle was applied by steadily increasing the oil pressure in the down-load ram system to a predetermined load or beam rotation and then a steady release to zero oil pressure in the system. A loading cycle was completed by a similar pressure increase and return to zero in the up-load ram system. Time required for a complete cycle was 12 min to 15 min.

After the programmed nine cycles were completed (Fig. 3), the loading was continued until either the specimen could no longer sustain a significant percentage of ultimate design load or the deflection capacity of the loading equipment was reached.

### TEST RESULTS

The performance of each test specimen is described in this section. Moment capacity at which yield of the reinforcement was first noted is reported for both upward and downward beam loadings. Ultimate moment and ductility of the assembly during the cyclic simulated earthquake loading is presented as a series of moment-rotation or moment-deflection curves. Reinforcement stresses during selected cycles are shown for a representative specimen. Maximum beam deflection and anchorage bond stress of beam reinforcement are also reported.

*General Behavior.*—Significant structural action observed in each test is summarized below for individual specimens.

*Specimen I.*—This specimen, representing an unconfined beam-column joint in a lower story of a tall building, was designed and detailed according to the Earthquake Manual to resist major earthquakes. Reinforcement details are shown in Table 1 and Fig. 4. Applied loads are listed in Table 2. The specimen maintained computed ultimate moment throughout the nine programmed load reversals illustrated in Fig. 3. Rectangular hoops in the joint developed stresses gradually during cyclic loading and were stressed to yield at the end of the test. The first diagonal hairline crack in the joint appeared during the first load cycle. Cracking increased until the surface concrete in the joint area became ineffective. At the end of the scheduled test, however, the column axial load was increased to the testing machine capacity of one million pounds. The column successfully carried this load which is 59% of computed ultimate column capacity and 55% greater than design.

*Specimen I-A.*—Strength and ductility of this specimen was similar to Specimen I even though it contained joint hoops with only one-half the cross-sectional area. The column loading was identical to that of Specimen I. During the second inelastic cycle, wide inclined cracks were observed crossing the sides of the joint. However, the specimen continued to demonstrate ductile behavior with a progressive small decrease in moment capacity. The beam developed 85% of computed ultimate moment at the end of the scheduled test.

*Specimen II.*—This specimen was nominally identical to Specimen I. A smaller column axial load simulating the probable actual load in a building was applied. This specimen carried the computed ultimate moment capacity of the beam throughout the test. Joint reinforcement details were satisfactory.

Some small vertical cracks in the joint area were noted during the third inelastic cycle. These cracks were attributed to a general bulging of the joint.

*Specimen III.*—This specimen was provided with a small column to represent upper stories of a building. It was anticipated that the specimen would develop a plastic hinge in the column when the beam load was applied in the down-ward direction. The specimen reacted as expected and developed the computed ultimate moment capacity of the column on the first plastic cycle. On the third cycle the joint area started to crack and the frame developed a

TABLE 2.—MOMENT CAPACITY

Specimen Number	Column Load $N$ , in kips	Beam Load, $F$	Calculated Moment Capacity (Actual Materials), in foot-kips		Test Moment <sup>b</sup> Applied at First Yield, in foot-kips		$\frac{M_{test}}{M_{calc}}$
			Beam $M_u$	Column $M_u$	Beam $M_b$	Column $M_c$	At Hinge
(a) 15-inch by 15-inch Columns							
I	644	Down	251.5	305	282	124.5	1.12
		Up	138	305	136	60.2	0.99
I-A	647	Down	233	305	248	109.5	1.06
		Up	128.5	305	140	62.0	1.09
II	284	Down	241	380	253	111.8	1.05
		Up	131	380	140	62.0	1.07
V	636	Down	247	305	220	97.2	0.89
		Up	137	305	147	65.0	1.07
V-A	649	Down	263	415	281	124.2	1.07
		Up	139	415	126	60.0	0.90
(b) 12-inch by 15-inch Columns							
III	335	Down	235	100	218	94.5	0.94 <sup>a</sup>
		Up	129.5	100	122	53.4	0.94
IV	30	Down	246	68.5	141	61.8	0.91 <sup>a</sup>
		Up	135	68.5	110	48.2	0.82

<sup>a</sup> Hinge in column; all others occurred in beam.

<sup>b</sup>  $M_b$  is at the column face and  $M_c$  is at the top of the beam.

<sup>a</sup> Hinge in column; all others occurred in beam.

<sup>b</sup>  $M_b$  is at the column face and  $M_c$  is at the top of the beam.

strength that was about half-way between that of the column and the column core. A fourth cycle produced only the ultimate moment capacity of the column core. Loss of the surface concrete on this small 12-in. by 15-in. column permitted sufficient eccentricity of the column load to cause horizontal displacement of the joint. This horizontal displacement caused additional eccentricity and the specimen became unstable. Test was terminated after the fourth cycle to prevent damage to the test apparatus. It should be noted that, in an actual building, structural response of a multicolumn frame would reduce the joint displacement that occurred in Specimen III.

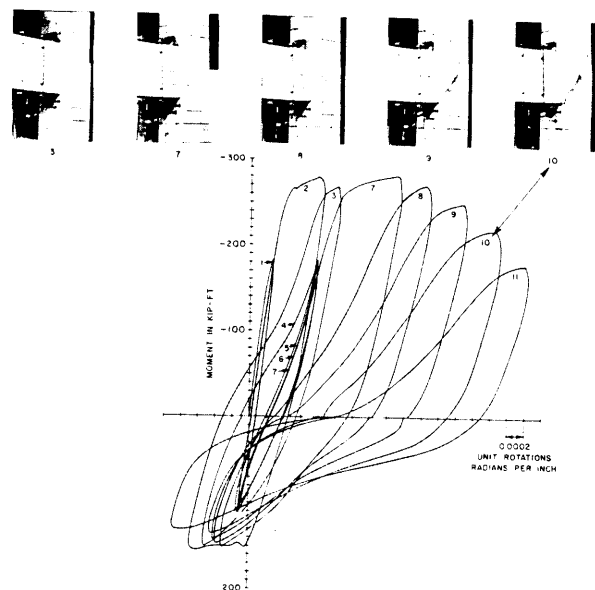


FIG. 8.—MOMENT-ROTATION CURVES FOR SPECIMEN I

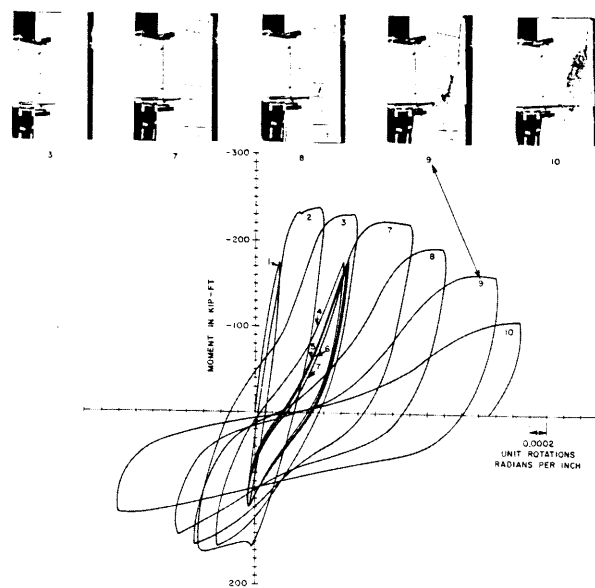


FIG. 9.—MOMENT-ROTATION CURVES FOR SPECIMEN IA

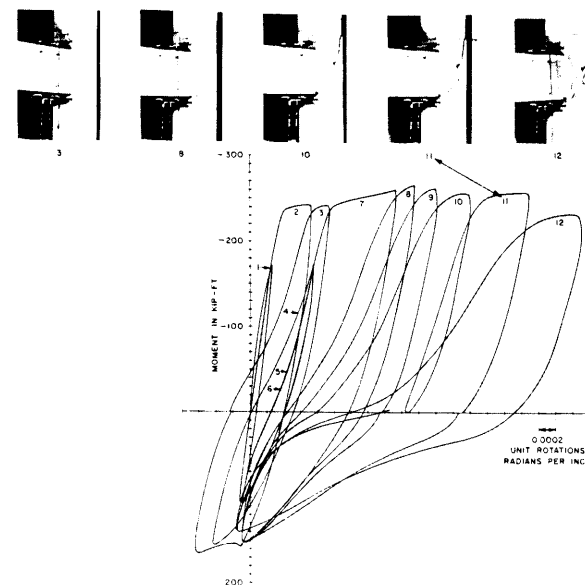


FIG. 10.—MOMENT-ROTATION CURVES FOR SPECIMEN II

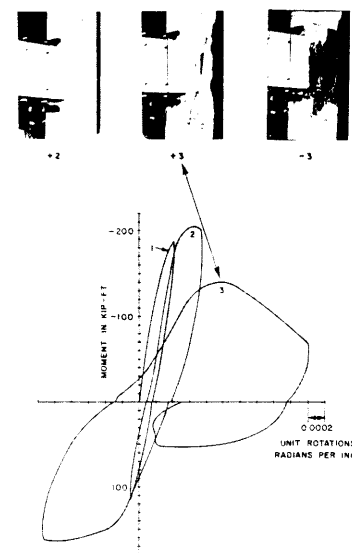


FIG. 11.—MOMENT-ROTATION CURVES FOR SPECIMEN V

steel. In the up-load half of this cycle, the two bottom bars reached yield stress and the flexure crack was open over the full depth of the beam. The crack at the bottom widened as yield strains developed to produce the ductility factor of 5.0. The top portion of the crack narrowed as compressive stress developed in the top four bars. This compressive stress did not reach yield. Consequently, the crack remained open from top to bottom after the load was returned to zero at the completion of cycle 2.

Reverse curvature of the moment-rotation plot was produced in the increasing load portion of the first half of cycle 3. The first portion of this curve is defined primarily by the compression stress-strain relationship of the bottom beam steel. The prior tension yielding of this steel produced a curvi-

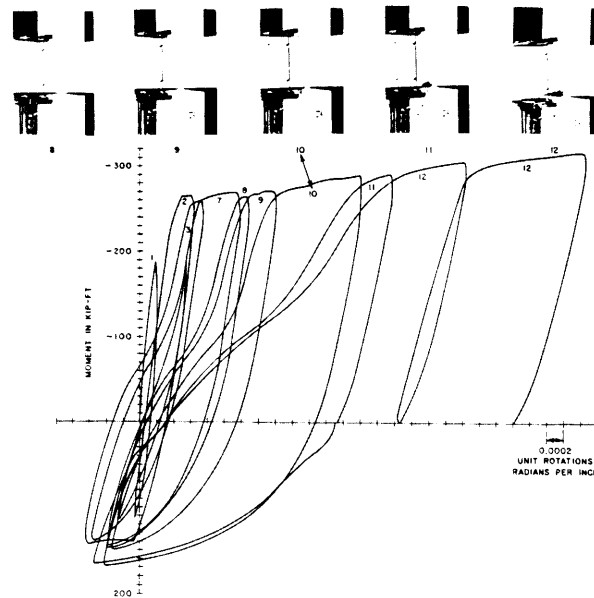


FIG. 12.—MOMENT-ROTATION CURVES FOR SPECIMEN VA

linear compression stress-strain relationship with an apparent reduction in beam stiffness. This "Baushinger effect"<sup>17</sup> caused the first reversal of beam load to generate a moment-rotation curve that is nonlinear and exhibits no sharp yield point. Yielding of the compression reinforcement permitted the bottom part of the crack to close, and the beam again acted as an ordinary cracked section. The remainder of the first half of the cycle was marked by reaching the yield moment, obtaining a ductility factor of 4.0 and finally unloading. The X-Y recorder traced a descending curve with a slope indicating a stiffness only slightly less than during the first elastic cycle loading. Therefore, the apparent loss of stiffness was recovered during this cycle.

The second half of cycle 3 was characterized by a sweeping curve resulting

<sup>17</sup>Singh, A., Gerstle, K. H., and Tulin, L. G., "The Behavior of Reinforcing Steel Under Reversed Loading," Material Research and Standards, American Society for Testing and Materials, Philadelphia, Pa., Vol. 5, No. 1, Jan., 1965, pp. 12-17.

from the "Baushinger effect" altering the stress-strain curves of both top and bottom beam steel.

Cycles 4, 5, and 6 were elastic cycles to 75% of yield moment in each direction. The first part of cycle 4 had a reverse curvature similar to the be-

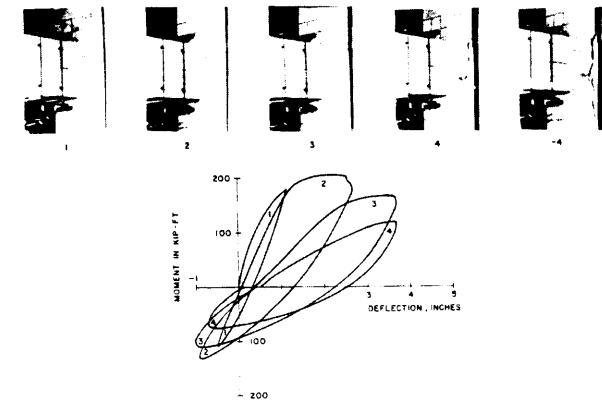


FIG. 13.—MOMENT-DEFLECTION FOR SPECIMEN III

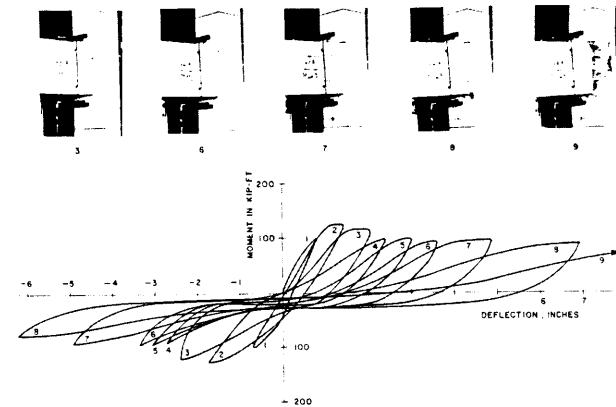


FIG. 14.—MOMENT-DEFLECTION FOR SPECIMEN IV

ginning of cycle 3. However, the "Baushinger effect" was only present for the first reversal of loading after a plastic excursion, so that the remainder of cycle 4 did not exhibit this effect. Cycles 5, 6, and the first half of cycle 7 did not show the "Baushinger effect" since the steel did not yield during this stage of loading. The remaining cycles followed the same pattern described for cycle 3.

TABLE 4.—BEAM DEFLECTIONS FOR DOWNWARD CYCLE

Test Number	Peak of Cycle Number	Beam Load, in pounds	Deflection Components, in inches						Deflection Measured, in inches $\Delta_{test}$	Comparisons, in percentage		
			Calculated		Measured		Total $\Delta_{comp.}$	Hinge (1) $\frac{Hinge(1)}{Hinge(1)+(2)}$		Hinge(1) $\Delta_{test}$	$\frac{\Delta_{comp.}}{\Delta_{test}}$	
			Elastic		Joint Distortion							
			Beam Hinge									
			Beam	Column	(1)	(2)						
I	1	18,500	0.29	0.13	0.28	0.13	0.83	—	0.94	68	29	88
	3	26,600	0.41	0.19	1.10	0.19	1.89	—	2.38	85	46	79
	7	28,400	0.44	0.20	1.92	0.43	2.99	—	3.88	82	49	77
	9	24,900	0.38	0.18	2.76	0.43	3.75	—	5.54	87	50	68
IA	1	17,400	0.26	0.12	0.26	0.02	0.74	0.06	0.92	93	28	81
	3	22,900	0.35	0.16	1.26	0.04	2.43	0.61	2.58	97	49	94
	7	22,000	0.33	0.15	1.73	0.07	3.51	1.23	4.10	96	42	86
	9	15,600	0.24	0.11	2.77	0.02	6.83	3.69	7.29	99	38	94
II	1	17,600	0.27	0.12	0.24	0.04	0.67	—	0.80	86	30	84
	3	24,200	0.36	0.17	0.99	0.13	1.65	—	2.04	88	48	81
	7	26,400	0.39	0.18	1.81	0.48	2.86	—	3.44	79	52	83
	9	26,400	0.39	0.18	2.35	0.63	3.55	—	4.46	79	53	80
V	1	18,700	0.29	0.13	0.43	0.07	1.15	0.23	1.18	86	36	98
	2	20,200	0.30	0.14	0.82	0.09	2.07	0.72	1.99	90	41	104
	3	13,400	0.20	0.09	2.14	0.04	6.39	3.92	6.49	98	33	96
VA	1	18,500	0.23	0.12	0.22	0.13	0.70	—	0.74	63	29	95
	3	25,900	0.32	0.17	0.67	0.22	1.38	—	1.54	75	43	90
	7	26,400	0.32	0.17	1.21	0.22	1.92	—	2.04	85	59	94
	9	26,600	0.33	0.17	1.69	0.41	2.60	—	2.64	81	64	99
III	1	17,600	0.27	0.26	0.39	0.04	1.16	0.20	1.04	91	37	112
	2	20,200	0.30	0.30	1.08	0.13	2.59	0.78	2.59	89	42	100
	3	16,300	0.24	0.24	1.62	0.11	3.64	1.43	3.61	94	45	99
	4	11,700	0.18	0.17	1.56	0.11	3.87	1.85	3.67	94	43	105
IV	1	9,700	0.15	0.17	0.19	—	0.80	0.29	0.74	—	25	108
	3	11,000	0.17	0.19	0.86	—	2.26	1.04	1.99	—	43	114
	7	9,200	0.14	0.16	2.31	—	4.62	2.01	4.79	—	48	96
	9	6,800	0.11	0.12	3.46	—	—	—	10.44	—	33	—

Shear force transmitted to the joint by beam loading was the primary cause of high stresses in the hoops. Therefore, the primary hoop design criterion should be diagonal tension caused by shear in the joint.

**Beam Deflections.**—The deflection of the specimen was measured at a point on the beam nine feet from the face of the column. Table 4 shows this deflection for selected down-loads for the various specimens.

Also shown in Table 4 is a tabulation of calculated and measured deflection components. The table can be used to identify sources of the resulting deflection to evaluate length of the plastic hinge zone and to examine validity of ductility factor. Three basic components are assumed to contribute to the deflection. As illustrated in Fig. 15, these components are the elastic deformation of the beam and column, rotation at the assumed beam hinge and shear distortion of the joint.

The elastic beam and column deflection components were calculated assuming a cracked section for the beam and uncracked section for the column. These calculated values do not include elastic deflection of the instrumented hinge region.

The designation Hinge (1) is used to identify deflection resulting from rotation occurring in the first 10 in. of beam length measured from the column

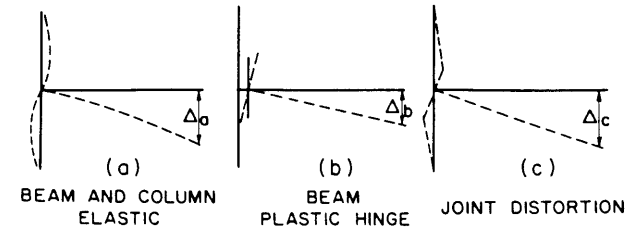


FIG. 15.—COMPONENTS OF BEAM DEFLECTION

face. This distance,  $l/2$ , in the region of highest beam moment is the primary plastic hinge zone. The designation Hinge (2) identifies deflection resulting from deformation in the second 10 in. of beam length. Some hinging does occur in this zone.

Joint distortion was measured by either the elongation of joint diagonals or by tangential displacement of the column rear face. In Tests III and IV, tangential displacement also included column plastic hinge action.

Comparison of deflections due to Hinges (1) and (2) provides information on the plastic hinging length. Note that cycle 1 is an elastic cycle but cycles 3, 7, and 9 include plastic yielding. If Hinges (1) and (2) were assumed to contain all of the beam plastic hinging action, then for the plastic excursions Hinge (1) supplied an average of 88% and Hinge (2) only 12%. Therefore, the assumption that most of the beam plastic hinging will occur in the primary  $l/2$  hinge zone was satisfactory.

Comparison of deflection contributed by Hinge (1) to total measured showed that about 30% to 60% of that occurring during excursions into the yield range was contributed by hinging in the first 10 in. The remainder was contributed primarily by joint distortion in all but two of the test specimens. In specimens III and IV plastic hinging in the column also contributed a significant

portion of the deflection. Based on these observations it is evident that rotation occurring in the primary plastic hinge zone  $t/2$  from the face of the column provides an extremely conservative estimate of the ductility factor.

**Anchorage Length of Beam Reinforcement.**—Stress in top beam reinforcement in the joint anchorage region is shown as plotted points in Fig. 16 for the six specimens which developed yield stress. The trend in any one case indicated that stress development was nonlinear, thereby indicating a non-uniform anchorage stress. Nevertheless, the general trend was toward development of full yield strength in the anchorage length provided. Although the steel yield zone penetrated into the columns in some of the tests, the bars did not show a serious loss in bond.

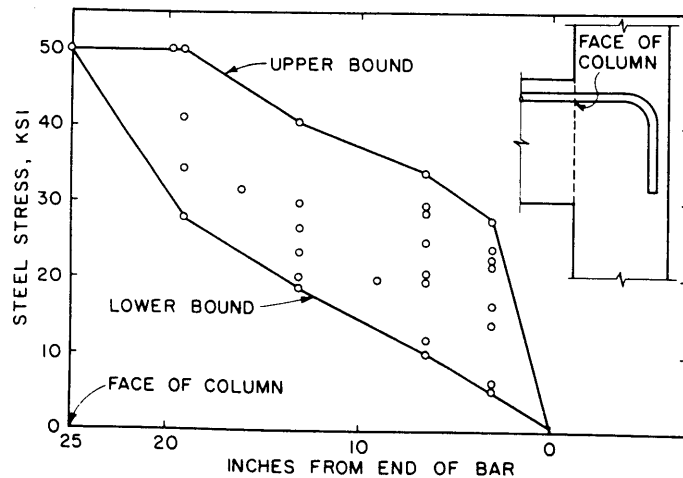


FIG. 16.—STRESS IN TOP BEAM REINFORCEMENT IN ANCHORAGE ZONE

Based on these test data, it appears that the ultimate bond stress formula, Eq. 4, used to compute anchorage length is adequate for use in earthquake resistant design of reinforced concrete structures.

**Analysis of Hoops.**—Two primary forces act on a beam-column joint. These forces are horizontal shear and vertical compression. Shear force is due to tension of beam reinforcement,  $f_y A_s$ , and horizontal external column shear,  $H$ , shown in Fig. 2 and illustrated in the beam-column joint of Fig. 17. The equation for shear force,  $V$ , in the joint may be expressed as

$$V = f_y A_s - H \quad (6)$$

The equation for moments acting on the joint section is

$$(f_y A_s) j d = (H) h \quad (7)$$

in which  $j$  = ratio of distance between centroid of compression and centroid of tension to the beam depth,  $d$ . All other terms are as previously defined. Since the column height,  $h$ , is much greater than  $j d$ ,  $f_y A_s$  is much greater than  $H$ .

From ACI 318-63, Section 1701 (e), the concrete shear force permitted for members subjected to axial load shall not exceed

$$V_c = 3.5 b d \phi \sqrt{f'_c} (1 + 0.002 N/A_g) \quad (8)$$

in which  $b$  and  $d$  are column dimensions shown in Fig. 17. A capacity reduction factor,  $\phi$ , of 1.0 was used for these test calculations. Other terms are as previously defined. Eq. 8 is applicable for all specimens.

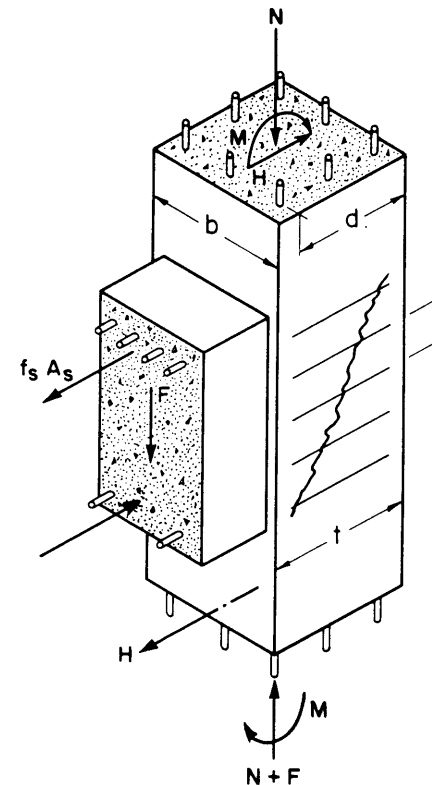


FIG. 17.—FORCES ON BEAM-COLUMN JOINT

For columns with low axial load, allowable concrete shear force calculated by ACI 318-63, Eqs. 17-2 and 17-3 will govern, so that

$$V_c = b d \phi \left[ 1.9 \sqrt{f'_c} + 2500 \frac{p V d}{M - N \frac{(4t - d)}{8}} \right] \quad (9)$$

in which shear,  $V$ , and moment,  $M$ , are maximum values calculated for the joint section of the column. Dimensions and section properties also pertain to the column.

Shear reinforcement is required for the difference between total shear force



to be resisted and that carried by the concrete, Eqs. 8 or 9. The cross-sectional area,  $A_v$ , of hoops (both legs) needed to resist this force is

$$A_v = \frac{s[V - V_c]}{\phi f_{yh} d} \dots \dots \dots (10)$$

Shear capacity, calculated by Eqs. 8 or 9 and 10 for each specimen, is listed in Table 5 as a percentage of the shear force that occurs in the joint under the application of the beam or column yield moment. The maximum moment obtained in the first (cycle 2) and last (cycle 9) scheduled inelastic excursion of the loading indicated in Fig. 3 is shown as a percentage of the ultimate moment calculated from Eq. 2 or Fig. 5 using actual material properties. It can be seen that the moment capacity of joints with low shear strength deteriorated rapidly. Conversely, joints with higher shear capacity developed their calculated ultimate moment and continued to maintain strength under re-

TABLE 5.—RELATIONSHIP OF CALCULATED CAPACITY TO MEASURED STRENGTH

Specimen Number	Joint Reinforcement	Column Load, in kips	Shear Capacity, <sup>a</sup> Percentage of Joint Shear at First Yield	Measured Moment, Percentage of $M_u$	
				Cycle +2	Cycle +9
(a) 15-inch by 15-inch Columns (Hinge in Beam)					
I	5 No. 4	644	87	112	105
IA	5 No. 3	647	79	106	76
II	5 No. 4	284	82	105	115
V	none	636	56	89	—
(b) 12-inch by 15-inch Columns (Hinge in Column)					
III	5 No. 4	335	67	94	—
IV	5 No. 4	30	74	91	58

<sup>a</sup> Includes both concrete and reinforcement

peated load reversals. For these tests, Eq. 10 with the capacity reduction factor equal to 1.0, provides a conservative calculation of the joint shear reinforcement.

These tests did not produce data concerning effectiveness of hoops in providing joint confinement for the ultimate axial load conditions assumed for Eq. 5. However, lateral restraint appears to be required to limit the bulging tendency produced by the combination of shear and axial load. Specimen V, containing a joint with no hoops, clearly showed the need for some joint confinement in order to develop initial ultimate capacity of structural members framing into an isolated joint. Specimen VA, containing no hoops but with confinement provided by members framing in on three sides, sustained the severe tests without any joint distress whatever.

Although the requirements for shear reinforcement and for confinement hoops for any one joint are not directly related, they are somewhat interdependent. Calculations of required hoops by Eq. 10 in various size beam-column joints show that the effect of shear is important for small columns but less significant for large columns. Conversely, calculations for column con-

finement based on Eq. 5 indicate that larger columns are more dependent on hoops to prevent bulging of the joint area.

## CONCLUSIONS

This series of tests demonstrates that properly designed and detailed cast-in-place reinforced concrete frames can resist moderate earthquakes without damage and severe earthquakes without loss of strength. Adequate energy absorption is provided by ductility of the reinforcing steel. Joints connecting beams and columns need special attention in design:

1. Hoops are required for unconfined (isolated) beam-column joints. A design procedure for hoops based on supplying adequate confinement and shear resistance will provide safe designs.
2. Corner joints with beams on only two column faces should be designed as unconfined joints requiring hoops until tests are made for this case.
3. Hoops are not required for exterior joints confined on at least three sides by beams or spandrels of approximately equal depth and meeting ACI 318-63 requirements for concrete strength needed to transfer the column load through the joint.
4. The cumulative ductility of a test specimen provided a measure of the ability of a structure to withstand seismic deformation. Well detailed joints sustained high values of cumulative ductility while they maintained their strength. Omission of important hoop reinforcement reduced amount of cumulative ductility which could be sustained.

These details of joint reinforcement are not limited to seismic design. Good design practice requires that joints be designed as strong as the adjoining members. These tests indicate that for the rare case of an isolated joint, a design for the usual forces of wind, dead, and live load will require hoops.

## ACKNOWLEDGMENTS

This investigation was made at the Structural Development Laboratory, Portland Cement Association under direction of E. Hognestad and W. G. Corley. Credit is due J. A. Sbarounis, E. H. Holland and staff of the Structural Bureau and Advanced Engineering Group, PCA Promotion Division, for their aid in planning and execution of the tests. The Seismology Committee, Structural Engineers Association of California, also contributed valuable guidance. A. G. Aabey, B. W. Fullhart, W. H. Graves, W. Hummerich and O. A. Kurvits skillfully performed the laboratory work.

## APPENDIX—NOTATION

The following symbols have been used in this paper:

$A_c$  = area of core of spirally reinforced or hoop tied column measured to the

outside of the spiral or hoop tie;

$A_g$  = gross area of spirally reinforced or tied column;

$A_s$  = area of tension reinforcement;

$A_s'$  = area of compression reinforcement;

$A_v$  = total area of web reinforcement within a distance,  $s$ , crossing a plane parallel to the longitudinal reinforcement;

$A_{sh}''$  = cross-sectional area of transverse, rectangular hoop reinforcement (both legs);

$b$  = width of compression face of flexural member;

$D$  = nominal diameter of reinforcing bar;

$d$  = distance from extreme compressive fiber to centroid of tension reinforcement;

$F$  = force applied at beam inflection point;

$f_y$  = yield stress of tension reinforcement;

$f_c'$  = concrete cylinder strength;

$f_y''$  = yield stress of transverse spiral reinforcement;

$f_{yh}''$  = yield stress of transverse rectangular hoop reinforcement;

$H$  = horizontal force on column;

$h$  = distance between column inflection points;

$h''$  = length of effective side of transverse rectangular hoop;

$j$  = ratio of distance between centroid of compression and centroid of tension to the depth,  $d$ ;

$k_1$  = a factor, 0.85 for  $f_c'$  up to 4000 psi and 0.80 for  $f_c'$  of 5000 psi;

$L$  = span length of beam;

$M_b$  = beam test moment measured at first yield;

$M_c$  = column test moment measured at first yield;

$M_u$  = ultimate moment capacity;

$N$  = applied column axial load;

$\rho = A_s/bd$  = tensile steel ratio;

$\rho_b$  = reinforcement ratio producing balanced conditions at ultimate moment;

$P_o$  = axial load capacity of actual member when concentrically loaded;

$P_u$  = column axial load capacity corresponding to  $M_u$ ;

$\rho' = A_s'/bd$  = compressive steel ratio;

$\rho'' = 0.45 (A_g/A_c - 1.0) f_c'/f_y''$ ;

$q$  = tension reinforcement index,  $\rho f_y/f_c'$ ;

$s$  = spacing of stirrups or hoops in a direction parallel to the longitudinal reinforcement;

$t$  = thickness of member;

$u$  = bond stress;

$V$  = total shear at section;

$V_c$  = shear force carried by concrete;

$\Delta H$  = horizontal displacement;

$\Delta V$  = vertical displacement;

$\mu$  = ductility ratio = ratio of rotation at ultimate load to rotation at yield load; and

$\phi$  = capacity reduction factor.